International Journal for Housing Science and Its Applications
Publish August 10, 2025. Volume 46, Issue 4 Pages 3085-3098

https://doi.org/10.70517/ijhsa464255

Research on digital preservation of wall paintings based on texture mapping and image reconstruction techniques

Xiaoqiang Tian[1] and Xiaosheng Ding[1,*]
[1] Dunhuang Academy, Lanzhou, Gansu, 736200, China
Corresponding authors: (e-mail: dhtt0937@163.com).

Abstract With the rapid development of digital technology, the digital preservation of murals has become an important means of cultural heritage protection. As immovable cultural heritage, frescoes face threats such as natural erosion and human damage. Traditional mural preservation methods are often difficult to fully capture the geometric features and texture details of murals, while modern 3D reconstruction and texture mapping techniques provide new possibilities for high-precision digitization of murals. In this study, the combination of texture mapping and incremental SFM algorithm is used to realize the complete digitization of geometric forms and texture details of murals by establishing the relationship between point cloud data and high-definition image data. The experimental results show that the processing time of the improved ISIFT feature matching algorithm on low-resolution mural images is 63.19 s, which is lower than the other four algorithms; in sparse point cloud construction, the incremental SFM algorithm has the highest accuracy with reconstruction error between 0 and 0.02, although it takes a relatively long time (1.7 s to 2.0 s); in dense reconstruction, the depth fusion method based on the dense In dense reconstruction, the number of point clouds generated by the depth fusion-based point cloud construction method is significantly higher than that of the SFS algorithm and the C/PMVS algorithm, and the results are more superior. In addition, the texture mapping and rendering technique proposed in this study nearly doubles the efficiency of the traditional mural splicing technique. The study confirms that the fresco digitization scheme proposed in this paper not only can preserve the geometric and textural information of frescoes more accurately, but also greatly improves the processing efficiency, which provides a precise and efficient technical path for the digital preservation and inheritance of frescoes.

Index Terms Mural digitization, texture mapping, image reconstruction, feature matching, point cloud construction

I. Introduction

As precious cultural heritage, murals have extremely important historical, artistic and cultural values. These murals record the life scenes, religious beliefs, artistic styles, heroic deeds and other information of the society, and have an irreplaceable role in the development of society, culture and art [1]-[3]. The creation of frescoes is skillful, rich in themes and diverse in styles, demonstrating the imagination and creative talent of artists, and has a high appreciation and research value [4]-[6]. The protection of murals is not only the treasure and inheritance of history and culture, but also the respect and esteem for human artistic creation.

Mural painting cultural heritage currently exists in a variety of diseases, such as armor, cracking, herpes, crispy alkali and dropsy, etc., and prone to the phenomenon of pigment layer shedding, fading and other phenomena, which may be due to changes in temperature and humidity, wind erosion, rainfall and other natural factors, carbon dioxide production, copying damage and other human factors [7]-[10]. Currently has stepped into the era of information technology, mural protection work to keep pace with the times, to keep pace with the times. Related cultural heritage protection workers should give full play to the role of digital technology, effectively build a scientific and perfect digital mural protection system, with the assistance of digital technology will be the mural information is complete, permanently preserved, and to achieve the digital virtual repair of murals, so that more people can truly experience the charm of the virtual display [11]-[13]. The practice of digital fresco protection has laid a solid foundation for the protection of frescoes, and can minimize the dangerous workability of the protection work of the relevant workers, so it is widely used in the protection of cultural heritage and creates a high realistic value [14], [15].

Texture mapping is the process of mapping a two-dimensional image or texture image onto the surface of a three-dimensional object. Image reconstruction techniques recover clear, high-quality images from damaged, blurred, or low-quality images and are essential for improving image quality and increasing the accuracy of image analysis. Texture mapping and image reconstruction techniques have a wide range of applications in computer graphics, by

enhancing image textures to increase realism and details, to obtain finer and more realistic scenes and characters, and have important applications in various cultural heritage preservation and restoration and other fields [16]-[18].

The preservation methods of frescoes range from chemical reagents to photo and video recording to the intervention of digital technology. In chemical preservation, literature [19] verified the ethanol solution of calcium hydroxyglycolate as a protective agent for frescoes, which not only fills the cracks, but also enhances the resistance to weathering. However, high concentrations of hydroxyglycolic acid are corrosive, and improper control of the concentration can easily cause irreversible diseases to the frescoes. Literature [20] confirms that although the mural curing agents - Paraloid B72 and transparent casein dispersant - have some protective properties, the effect of the two curing agents is greatly reduced under the production of black fungi. Similarly, literature [21] evaluated the effectiveness of Pepe Ostar Gold matte pictorial varnish and Paraloid B72 as protective coatings for frescoes in accelerated aging tests over a certain period of time, but since both are acrylic-based polymeric materials, they were stable for a maximum of only 8 years.

Excessive from chemical protectants to image recording improves the efficiency of fresco preservation, when the basic camera equipment recorded two-dimensional images of frescoes are prone to lose part of the information, such as the dome frescoes rendered by two-dimensional images are severely deformed [22]. Although the literature [23] proposed a high spatial resolution mural preservation method by fusion of close-up photogrammetry and mapping techniques, which was acquired by a mirrorless Sony Alpha 7 III camera, and then image processing was carried out to construct a mural painting database. However, this method is difficult to visualize the texture of the fresco pigment layer and the surface of the fresco material layer. Entering the stage of digital technology, literature [24] combined hyperspectral imaging technology, continuous spectrum removal and histogram stretching for mural image processing, and this method could identify the pigment and the mural information in the lower layer of the pigment, and carried out a virtual restoration of the mural as a way of obtaining digital conservation. Literature [25] accomplished the restoration of frescoes by digital image processing techniques, generative adversarial networks and self-attention mechanisms, and performed super-resolution 3D reconstruction to obtain stronger conservation effects.

As an important witness of human civilization, murals carry rich historical information and artistic value. However, due to the erosion of the natural environment, the destruction of human factors, and the aging of the materials themselves, many precious murals are facing the increasingly serious threat of destruction. Traditional mural protection methods mainly rely on field restoration and plane photographic records, these methods can not fully preserve the geometric features, texture details and spatial location of the mural, restricting the effective protection and inheritance of the mural cultural heritage. With the development of digitization technology, three-dimensional reconstruction and texture mapping technology provide a new technical way for the high-precision digital preservation of frescoes. Nevertheless, the digitization of mural paintings still faces many challenges: the complex surface texture of mural paintings is easily affected by lighting conditions, which leads to the difficulty of feature point extraction and matching; the cumulative error in the process of 3D reconstruction results in the decrease of model accuracy; and the color distortion due to the change of viewing angle in the process of texture mapping. Existing research mostly focuses on improving a single technical link, and lacks a systematic solution for digitizing murals, which cannot meet the high-precision requirements for digitizing murals for protection. Based on this, this study proposes a fresco digitization preservation method based on texture mapping and image reconstruction techniques, with the goal of realizing high-precision 3D reconstruction and texture recovery of frescoes. In this paper, we first collect and preprocess the mural texture information with high precision, design a reasonable shooting layout to ensure sufficient overlap between images, and perform geometric correction, leveling and stitching on the collected point cloud data and image data. In the mural image reconstruction stage, the study proposes an improved ISIFT algorithm to improve the accuracy and efficiency of feature point matching, adopts the incremental SFM algorithm to construct a sparse point cloud, generates a dense point cloud through depth map fusion, and introduces line-of-sight weights to optimize the 3D surface model. For mural texture mapping, this paper proposes a texture selection strategy based on image quality assessment, and achieves seamless texture fusion by energy minimization method. In order to verify the effectiveness of the proposed method, the study compares and analyzes the performance of different feature matching algorithms, point cloud construction methods and texture mapping techniques in mural digitization. The experimental results show that the fresco digitization scheme proposed in this paper not only excels in model accuracy and texture quality, but also significantly improves the processing efficiency. The innovation of this study is to construct a complete fresco digitization technology chain from data acquisition to 3D reconstruction to texture mapping, optimize the algorithm for the unique texture characteristics and geometric features of frescoes, and provide systematic technical support for the digital protection and inheritance of frescoes. Through this study, the original appearance of frescoes can be preserved more realistically and accurately, providing

high-quality digital resources for subsequent virtual display of frescoes, educational communication and academic research, and further promoting the technological development of cultural heritage digital protection.

II. Digitization programme for wall paintings combining texture mapping and image reconstruction

II. A. Acquisition and pre-processing of mural texture information

II. A. 1) Acquisition of mural texture information

Texture mapping is an important part of the work of digital three-dimensional modeling, texture information restores the original appearance of the real world, expresses more detailed information about the details of the artifacts, and facilitates the extraction of characteristics such as the type and extent of the disease. Image picture acquisition and processing is also a very important work, it directly affects the final model effect. Due to the acquisition of the entire mural point cloud data, only by the scanner itself to obtain the image data can not meet the needs of the actual work, so it must be additional to obtain higher quality image data. For this reason, it is necessary to set up a reasonable camera shooting layout to achieve a satisfactory degree of photo overlap, the overlap between neighboring images needs to be at least 30% in order to produce an orthophoto map. Camera shooting stations were added to the scanner stations to ensure sufficient overlap between images, and a tripod was used to fix the camera, which not only prevented parallax, but also ensured the overlap between multiple images. At each station, camera shots were taken from three angles, horizontally and vertically. The angle between shots taken with the camera placed horizontally depends on the FOV (field of view) of the camera lens. This shooting scheme ensures that there is sufficient overlap between the photos in the horizontal and vertical directions.

II. A. 2) Pre-processing

(1) Point cloud data pre-processing

Due to the scanner in the field use of the complex working environment, people walking, trees, buildings blocking, construction dust and scanning the target itself reflective properties of the uneven and other impacts will cause the scanning of the point cloud data obtained by the unstable points and noise points, noise points generated by many reasons, mainly the following three:

(a) Noise generated by the surface factors of the scanned object, such as the surface roughness, ripples, surface material and other errors. This is because the laser scanner is the use of laser as a means of measurement, so when the surface of the object being photographed is darker, i.e., lower reflectivity, most of the incident light will be absorbed, in addition to the scanning distance is farther away, the incident laser reflected light signal is weaker in the case is also very easy to produce noise.

(b) Errors caused by the scanner itself, such as the measurement accuracy of the laser scanner, scanning resolution and scanner vibration caused by the error.

(c) accidental noise, this noise refers to the scanning process due to some accidental factors caused by the scanning data errors, such as in the scanning of the building, there are vehicles or pedestrians in the scanner and the building being scanned between the passage, so that the scanning of the data obtained by the data is the wrong data, it should be filtered or deleted, that is, data filtering.

(2) Image data preprocessing

Generally speaking, it is necessary to carry out the basic processing of the original image in the following aspects:

(a) Geometric correction. Remove the geometric distortion of the digital image caused by the camera. Geometric correction is necessary for us to get quantitative spatial measurement data from the digital image, and only after correction can we interpret its content.

(b) Leveling of tilted digital images. When using a digital camera to obtain digital images, it is difficult to ensure that the camera's three spatial rotation axes are horizontal or vertical, resulting in the imaging plane and topographic map plane is not parallel, resulting in geometric shape changes, such as a circle into an ellipse, so there is a need to flatten the tilted digital image into a horizontal image.

(c) Digital image stitching. With a digital camera to take digital images of topographic maps, it is necessary in the computer, the split image splicing, in order to facilitate the analysis and processing. Inclined digital image leveling, which is a typical projection problem, as shown in Figure 1, S is the center of photography, in a prescribed object-square spatial coordinate system whose coordinates are (X_s, Y_s, Z_s), M for any ground point, which has the object-square spatial coordinates of (X, Y, Z), m for the M in the Image P on the composition, photography, S, m, M three points are located in a straight line. Let x, y be the image space coordinates, X_m, Y_m, Z_m be the image space auxiliary coordinates, then by the covariance condition:

$$\begin{cases} (x - x0)/(-f) = (a1 \cdot Xm + b1 \cdot Ym + c1 \cdot Zm)/(a3 \cdot Xm + b3 \cdot Ym + c3 \cdot Zm) \\ (y - y0)/(-f) = (a2 \cdot Xm + b2 \cdot Ym + c2 \cdot Zm)/(a3 \cdot Xm + b3 \cdot Ym + c3 \cdot Zm) \end{cases} \tag{1}$$

Where $(x0, y0)$ are the coordinates of the image principal point, and f is the focal length of the digital camera lens. $ai, bi, ci(i = 1, 2, 3)$ is the 9-direction cosine of the 3 outer azimuthal elements of the image. Before the transformation can be translated coordinates, the midpoint is located in the middle of the image plate, so that it can be considered: $x0 = 0, y0 = 0$. And take f (focal length) as an approximation of Zm, then the above company formula can be simplified as:

$$\begin{cases} x = -f \cdot (a1 \cdot Xm + b1 \cdot Ym + c1 \cdot Zm) / (a3 \cdot Xm + b3 \cdot Ym + c3 \cdot f) \\ y = -f \cdot (a2 \cdot Xm + b2 \cdot Ym + c2 \cdot Zm) / (a3 \cdot Xm + b3 \cdot Ym + c3 \cdot f) \end{cases} \tag{2}$$

The image leveling algorithm is simple and easy to implement.

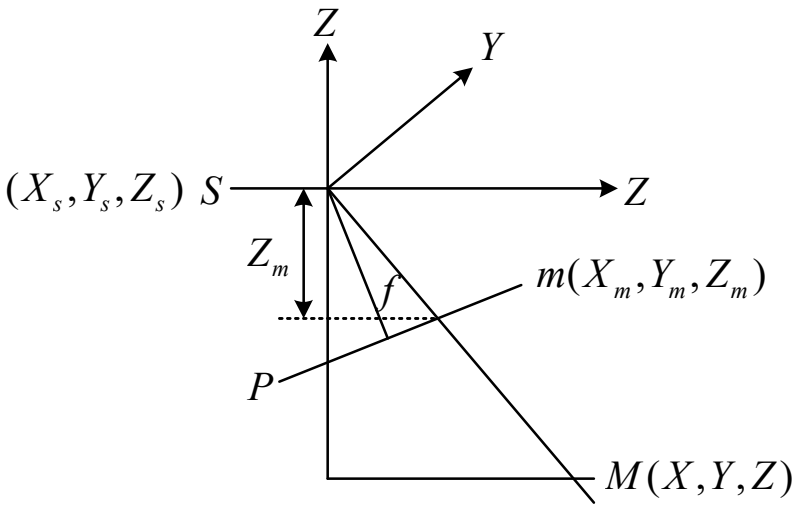

Figure 1: Schematic diagram of projection method

Image stitching can be performed on images that have been processed through geometric correction and leveling. The algorithm for image stitching is as follows:

a) Separately select points with the same name on image a and image b to be spliced to form control point sets Sa and Sb.

b) Take image a as the master spliced image and image b as the slave spliced image.

c) Select two pairs of homonymous points: $P1$, $P2$ and $P_1^{'}$, $P_2^{'}$, the splicing method is different, and the way of selection is also slightly different, and select $P1$, $P1$ that satisfy the following conditions: for any two points P_i, P_j, $P_i \in Sa \,\&\, P_j \in Sa$, $abs(P1y * P2y) \geq abs(P_i y - P_j y)$.

d) Find the rigid transformation based on $P1$, $P2$ and $P_1^{'}$, $P_2^{'}$: $X = Ax + by + cy = Dx + Ey + F$.

e) Based on the collocation method and the rigid transformation formula, select the auxiliary control points and add them to the set of Sa, Sb:

f) Perform multiple linear regression analysis on the control point pairs of Sa, Sb to find the affine transformation coefficients A0, A1, A2, B0, B1, B2. i.e.:

$$\begin{gathered} Pi^{'}, Pi, Pi^{'} \in Sa \,\&\&\, Pi \in Sb \\ Pi^{'}.x = A0 \cdot Pi.x + A1 \cdot Pi.y + A2 \\ Pi^{'}.y = B0 \cdot Pi.x + B1 \cdot Pi.y + B2 \\ (i = 0, 1, \cdots, n-1) \end{gathered} \tag{3}$$

In order to minimize q according to the principle of least squares:

$$q = \sum \left[Pi^{'} \cdot x - (A0 \cdot Pi \cdot x + A1 \cdot Pi \cdot y + A2) \right]^2 (i = 0, 1, \cdots, n-1) \tag{4}$$

The regression coefficients A0, A1, A2 should satisfy the following equations:

$$CC^{\acute{u}} = \begin{bmatrix} A_0 \\ A_1 \\ A_2 \end{bmatrix} = C \begin{bmatrix} x_0 \\ x_1 \\ \cdots \\ x_{n-1} \end{bmatrix} \tag{5}$$

Of these, $x_i = P_i x$, $y_i = P_i y$:

$$C = \begin{bmatrix} x_0 & x_1 & x_2 & \cdots & x_{n-1} \\ y_0 & y_1 & y_2 & \cdots & y_{n-1} \\ 1 & 1 & 1 & \cdots & 1 \end{bmatrix} \tag{6}$$

Solve the above equations using Cholesky decomposition method to get the regression coefficients A0, A1, A2, and similarly, the regression coefficients B0, B1, B2 can be obtained.

g) If it is an indexed color image, it is necessary to analyze the two index tables of image a, b, try to find out their similar color values, and merge the index tables of image a, b to form a new index table.

h) Image resampling, taking into account the two main factors of speed and effect, the bilinear interpolation method is used for resampling, and the coordinate point $P'(x', y')$ in the spliced image is coordinate transformed:

$$\begin{aligned} x &= A0 \cdot x' + A1 \cdot y' + A2 \\ y &= B0 \cdot x' + B1 \cdot y' + B2 \end{aligned} \tag{7}$$

(x, y) is the coordinate point in the original imageb.

Rounding operation is performed on x, y to obtain:

$$\begin{aligned} m &= \text{int}(x) \\ n &= \text{int}(y) \\ C &= x - m \\ D &= y - n \end{aligned} \tag{8}$$

Among them, $0 \le C \le 1, 0 \le D \le 1$. Take the example of grayscale image resampling:

$$\begin{aligned} g(x', y') = (1-C) \cdot (1-D) \cdot g(m,n) + C \cdot (1-D) \cdot g(m+1,n) \\ +(1-C) \cdot D \cdot g(m,n+1) + C \cdot D \cdot g(m+1,n+1) \end{aligned} \tag{9}$$

Where $g(x', y')$ is the value of the corresponding sampled grayscale image at the point (x', y') in the spliced image. The advantage of this interpolation method is that it is fast and effective, but the disadvantage is that it results in a slight loss of resolution in the spliced image. Other types of images (e.g., binary images, indexed images, true-color images) are, in principle, resampled using the transform formula.

II. B.Wall painting image reconstruction

The first stage of mural image reconstruction is to reconstruct the corresponding 3D model by adopting the image set, and the second stage is to generate the 2D panorama from the 3D model. In this subsection, the 3D reconstruction process from the step of generating the matching points of image features to the step of texture mapping and color fusion will be described in detail.

II. B. 1) Image feature point extraction and matching

(1) Scale space construction

Scale space is the concept used to obtain the characteristics of the image under different scale changes, which uses the Gaussian convolution kernel function to realize the scale space transformation, as shown in Eq. (10), in which the Gaussian kernel function $G(m,n,\sigma)$ is the computation method shown in Eq. (11), and its convolution of the image coordinates $I(m,n)$ is computed to derive the scale space $L(m,n,\sigma)$, where σ denotes the Gaussian normal distribution standard deviation value. For:

$$L(m,n,\sigma) = G(m,n,\sigma) * I(m,n) \tag{10}$$

$$G(m,n,\sigma) = \frac{1}{2\pi\sigma^2} e^{-(m^2+n^2)/2\sigma^2} \tag{11}$$

Different scale space parameters σ will get different degree of smoothness of the image, then constructed a different scale space [26], [27]. SIFT algorithm in the basic scale space concept, the introduction of Gaussian difference scale space concept, Gaussian difference scale space is obtained by the difference of the image in different scale space, such as formula (12):

$$\begin{aligned} D(m,n,\sigma) &= L(m,n,k\sigma) - L(m,n,\sigma) \\ &= (G(m,n,k\sigma) - G(m,n,\sigma)) * I(m,n) \end{aligned} \tag{12}$$

(2) Scale space peak solving

On the basis of constructing the scale space pyramid, we can solve for the point that has obvious characteristics in the relative local range and is still the peak at different scales, which is called the peak point.

(3) Localization of feature points

The curvature of these points in the Gaussian differential scale space is asymmetric, and the Taylor expansion of the Gaussian differential scale space function can be obtained as Eqs. (13) and (14). For:

$$D(x) = D + \frac{\partial D^T}{\partial x}x + \frac{1}{2}x^T\frac{\partial^2 D}{\partial x^2}x \tag{13}$$

$$\hat{x} = -\frac{\partial^2 D^{-1}}{\partial x^2}\frac{\partial D}{\partial x} \tag{14}$$

The derivation of formula (13) to get formula (14), so that it is equal to 0, you can find the location of the extreme value, using the value of the substitution of formula (13) to calculate to get $D(x)$, if the value meets the formula 3-6 is a qualified characteristic point. For:

$$|D(\hat{x})| \geq 0.03 \tag{15}$$

(4) Orientation Matching

This step implements the feature rotation invariant property of the SIFT algorithm and will compute the gradient m of each of its feature points as well as the direction of the gradient θ for a smooth image L on a certain scale, as shown in Eq. (16) and Eq. (17), respectively. For:

$$m(x,y) = \sqrt{(L(x+1,y)-L(x-1,y))^2 + (L(x,y+1)-L(x,y-1))^2} \tag{16}$$

$$\theta(x,y) = tan^{-1}((L(x,y+1)-L(x,y-1))/(L(x+1,y)-L(x-1,y))) \tag{17}$$

(5) Feature descriptor construction

After obtaining the gradient directions of individual points, the local image descriptor of SIFT feature points consisting of 128-dimensional neighborhood gradient directions can be constructed.

II. B. 2) Incremental SFM-based sparse point cloud construction

SFM (recovery in camera motion) is a growing reconstruction process. It starts the reconstruction from the initial two views and minimizes the cumulative error by using beam method squaring to generate an optimal sparse point cloud scene [28]. Using SFM to restore the target scene optimizes the camera intrinsic and extrinsic parameters as well as the 3D points in space. As shown in Eq. (18), the ordinate i denotes the i th picture, x_j denotes the j th point in the scene, x_j^i denotes the projection of the 3D point X_j on the i th picture, and P_i is the camera projection matrix for the given $\{X_j, P_i\}_{i,j}$ relation to minimize its reprojection error:

$$\min_{\{P_i\}_i,\{X_j\}_j} imize \left\| \sum_{j=0}^{m}\sum_{i=0}^{n} x_j^i - P_i X_j \right\|_2 \tag{18}$$

II. B. 3) Generating dense point clouds based on depth map fusion

(1) Stereo image pair selection

The selection of stereo image pairs is not only important for the accuracy of stereo visual matching, but also affects the final generated point cloud results.

(2) Depth map calculation

Denote I_i as the i th input image in the image set, I_j as its corresponding reference image, and the associated cameras $\{K_i, R_i, C_i\}$ and $\{K_j, R_j, C_j\}$, the are the intrinsic parameters, rotation matrix and camera center, respectively. Firstly, each pixel $p(u,v,1)^T$ in I_i is randomly assigned to a 3D plane, and Eq. (19) can be obtained from the camera geometric model, where λ is a random value in the range:

$$X_i = \lambda K_i^{-1} p \tag{19}$$

Let the projection matrix of the two cameras be $P_i = [I_{3\times3} \mid 0_3]$, $P_j = [R \mid t]$ and a plane satisfying $\pi^T X = 0$, where $\pi = (V^T, 1)^T$ and from the plane we can obtain the single response matrix H as shown in Eq. (20):

$$H = R - tV^T \tag{20}$$

Through the camera projection matrix with plane parameters Eq. (20) can be rewritten as:

$$H_{ij} = K_j\left(R_j R_i^{-1} + \frac{R_j(C_i - C_j)n_i^T}{n_i^T X_i}\right)K_i^{-1} \tag{21}$$

A rectangular window B of size $\omega \times \omega$ is placed around the pixel p, and for each pixel point q within this rectangle, its corresponding pixel point in the image H_{ij} is found through the single response matrix I_j. The aggregation matching error value can be obtained by normalized correlation value (NCC) as in equation (22):

$$m(p, f_p) = 1 - \frac{\sum_{q\in B}(q-\overline{q})(H_{ij}(q) - \overline{H_{ij}(q)})}{\sqrt{\sum_{q\in B}(q-\overline{q})\sum_{q\in B}(H_{ij}(q) - \overline{H_{ij}(q)})^2}} \tag{22}$$

After initialization, each pixel point on the image I_i is associated with a 3D plane, which is randomly assigned for the optimization of the plane f_p to further reduce the error value of the plane f_p by adjusting the parameter values of the associated plane.

(3) Depth map optimization

For each point $p(u,v,1)^T$ on the image I_i, it is reflected to a 3D point $P(x,y,z,1)^T$ in 3D space by the depth value of the point α and the parameters of the camera:

$$P = \alpha R_i^T K_l^{-1} p + C_i \tag{23}$$

After the point P is computed, the 3D point is projected onto the set of neighboring images N^i of the image I_t, and if N_k^i is the k th image of it, then define $d(X,N_k^i)$ as the depth value of P with respect to the camera N_k^i, and define $\alpha(P,N_k^i)$ is the depth value computed after P is projected onto the image I_i. When these two values satisfy the formula, it means that P is depth-consistent on the image N_k^i, and when more than four images satisfy this condition, it means that P is a reliable 3D scene point.

$$\frac{|d(X,N_k^i)-\alpha(P,N_k^i)|}{\alpha(P,N_k^i)} < 0.01 \tag{24}$$

After the above filtering method, the error will be minimized and the noise will be removed from the depth map of each view.

(4) Depth map fusion

The pixels in the depth map of camera C_i are back-projected into the space to obtain the 3D point P, the 3D point P is again projected onto the neighboring camera $C_\#$ of C_i and the depth of this projection on the neighboring camera $\alpha(X,C_\#)$ is calculated, if this value is greater than the depth value $d(X,C_\#)$ of point P with respect to camera $C_\#$, then the projection of point P is considered to be obscured can be eliminated, if the two depth values are satisfied:

$$\frac{|d(X,C_\#)-\alpha(X,C_\#)|}{\alpha(X,C_\#)} < 0.01 \tag{25}$$

Then it means that the projection of point P in the neighboring camera is duplicated redundant information and the point needs to be eliminated from the neighboring camera. Finally, the depth map corresponding to each view is mapped into 3D space and merged into a dense point cloud with a larger number of 3D points.

II. B. 4) 3D surface modeling and its optimization

Surface reconstruction is actually the process of mesh construction of points in a point cloud, which centers on constructing discrete points into a continuous surface. Let the tetrahedral ensemble of the input 3D point set after tetrahedralization be T, and the free space support of the tetrahedron T be $f(T)$, which is obtained by summing up the weights of all the lines of sight through which the tetrahedron T passes as shown in Eqn. (26), where $\alpha(p)$ is the weight of the point p. For:

$$f(T) = \sum_{(c,p)\in\{(c,p)\in S|(c,p)\cap T\neq\varnothing\}} \alpha(p) \tag{26}$$

By estimating the variation of $f(T)$ values of the line of sight within the vicinity of the point p, the presence of noise can be detected efficiently and the effect of noise can be reduced. In Eq. (27) k denotes the interval $[0,k]$ and $f_{cp}(x)$ records the degree of free space support of the line of sight through each tetrahedron.

$$\gamma(k) = \frac{(\max(f_{cp}(x)\,|\,x\in[0,k]))}{2} + \frac{(\min(f_{cp}(x)\,|\,x\in[0,k]))}{2} \tag{27}$$

II. B. 5) Texture Mapping and Rendering

Firstly, the visual information of the input data is processed, for the triangular mesh facet F_i has l_i as its associated viewpoint image texture, and the energy formula is constructed for the neighboring facets F_i and F_j as shown in Eqs. (28) and (29). Where E_{data} is F_i the quality of the texture on l_i by summing the gradient magnitude $\nabla(I_{l_i}(p))$ of all pixels in the region $\varphi(F_i,l_i)$, where $\varphi(F_i,l_i)$ is the reprojected region of F_i on l_i. E_{smooth} minimizes the differences between the images as shown in Eq. (30):

$$E(l) = \sum_{F_i\in Faces} E_{data}(F_i,l_i) + \sum_{(F_i,F_j)\in Edges} E_{smooth}(F_i,F_j,l_i,l_j) \tag{28}$$

$$E_{data} = -\int_{\phi(F_i,l_i)} \|\nabla(I_{l_i}(p))\|_2 dp \tag{29}$$

$$E_{smooth} = [l_i \neq l_j] \tag{30}$$

Then Eq. (31) can minimize the color difference between neighboring triangular facets and minimize the color difference between neighboring vertices within the same texture block:

$$\arg\min_{g} \sum_{v} (f_{v_{left}} + g_{v_{left}} - (f_{v_{right}} + g_{v_{right}})^2 + \frac{1}{\lambda} \sum_{v_i, v_j} (g_{v_i} - g_{v_j})^2 \tag{31}$$

III. Analysis of the mural digitization programme

III. A. Image feature point extraction and matching analysis

III. A. 1) Preparation of analytical experiments

The purpose of the experiments in this section is to compare the improved algorithm SIFT with the classical algorithms for feature point matching, SIFT (scale invariant features), SURF (speeded up robust features), ORB (oriented rapid rotated brief features), and SC-RANSAC (random sampling consistency), and to examine the performance of ISIFT (scale invariant features with the introduction of Gaussian difference) in terms of the time of feature matching, feature matching point performance in terms of the time of feature matching, the number of feature matching points, and the error of feature matching.

III. A. 2) Analysis of experimental results

The above five algorithms are used to feature match 200 pairs of overlapping mural images in the mural dataset, and the time of feature matching, the number of feature matching points, and the feature matching error of each type of algorithm on the mural image pairs are recorded respectively. Since the one-shoulder transformation matrix between image pairs in the mural dataset is known, the symmetric transfer error can be used to evaluate the matching accuracy of each algorithm. Here the symmetry transfer error is calculated for each pixel in the fresco image. In order to evaluate the error distribution of each algorithm, the (0.01~0.2) pixel range is divided into 19 equally spaced intervals such as 0.01~0.02 at 0.01 intervals in the experiments, while two larger special intervals of 0.200~1.000 and >1.000 are added to count the outlier values, and the average errors of the five algorithms for each pair of mural images are recorded separately for each interval of the percentage of the number of mural images, as shown in Fig. 2. The horizontal axis in Fig. 2 indicates the statistical intervals of the average error, and the vertical axis indicates the number percentage of the error distribution. The experimental data show that the error of ISIFT is almost always less than 0.0425 pixels and is better than all other methods. Table 1 shows the statistics of the number of minimum average error images obtained by the five algorithms on the dataset. The data shows that ISIFT produces smaller feature matching errors on most of the mural images than the other 4 algorithms.

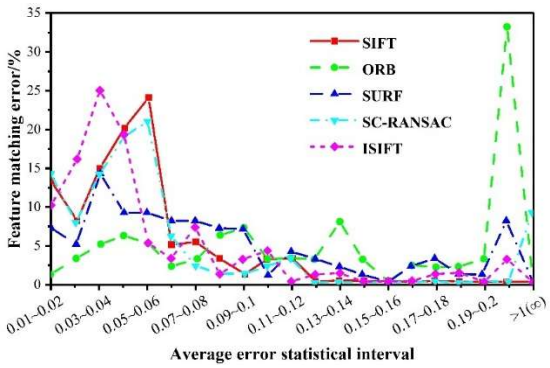

Figure 2: Feature matching error distribution

Table 1: Minimum average error number of images

Algorithm	Minimum average error number of images
SURF	15
SIFT	12
SC-RANSAC	15
ORB	0
ISIFT	87

The number of correct matching points obtained by the five algorithms is shown in Fig. 3, and the running time of the five algorithms is shown in Fig. 4, where (a)~(b) are 10244×7715 pixels and 5079×3711 pixels, respectively. Since there are two resolutions of mural images in the mural dataset, the experimental data are categorized in this

paper, and from the experiments, it can be concluded that the ISIFT algorithm is able to obtain the maximum number of matching points with the least running time on the higher resolution (10244×7715 pixels) mural image with richer texture, and it can be concluded that ISIFT algorithm can achieve the highest number of matching points in the mural image with less texture and lower resolution (5079×3711 pixels) mural images, not only can it obtain better accuracy and number of matching points more stably, but also its average processing time of 63.19s is lower than the other four algorithms.

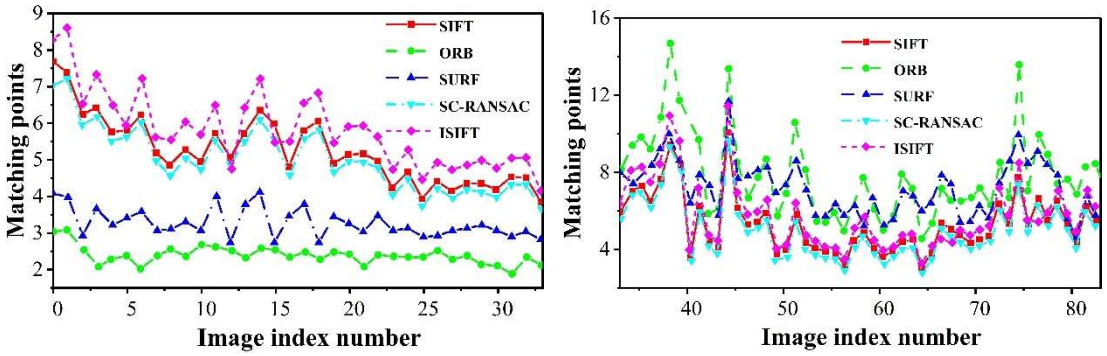

(a)10244× 7715 pixels (b)5079× 3711 pixels

Figure 3: The correct matching points obtained by five algorithms

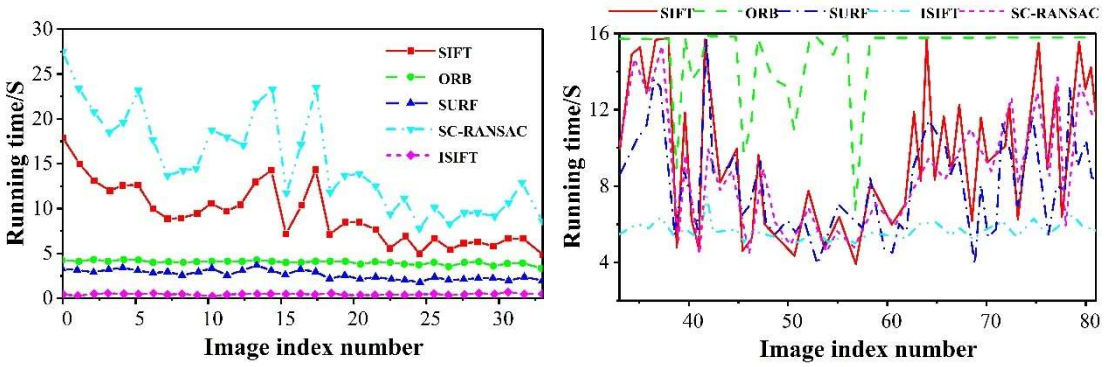

(a)10244× 7715 pixels (b)5079× 3711 pixels

Figure 4: The running times of five algorithms

III. B. Analysis of sparse point cloud construction based on incremental SFM

III. B. 1) Experimental environment

This experimental platform is a personal computer with a 12th Gen Intel Core i9-12900K CPU, NVIDIA GeForce RTX 3070 GPU, DDR4 3600MHz 8GB*2 RAM, and 500G mechanical hard disk.

III. B. 2) Experimental setup

This chapter compares and validates the incremental, holistic and hybrid SFM algorithms, verifies the superiority of the incremental SFM algorithm proposed in this paper in sparse point cloud construction, and demonstrates and analyzes the final dense model, six mural images (A, B, C, D, E, F) are selected from the dataset above as the experimental objects in this subsection.

III. B. 3) Data analysis

Figure 5~Figure 6 shows the comparison of error and running time of the three SFMs, respectively. In Figure 5~Figure 6, the error of incremental SFM, holistic SFM and hybrid SFM are denoted as E1, E2 and E3, respectively, and the running time of incremental SFM, holistic SFM and hybrid SFM are denoted as T1, T2 and T3, respectively, and the value of 0 in the figure denotes the reconstruction failure. The hybrid SFM reconstruction fails because it cannot complete the subset division. From the data in the table, it can be seen that in terms of running time, incremental SFM has the longest reconstruction time, holistic SFM has the shortest reconstruction time, and hybrid

SFM reduces the reconstruction time by more than 5% in comparison with incremental. Incremental SFM takes the most time (1.7s~2.0s) because it increments the mural images one at a time and performs triangulation and beam leveling once for each newly registered mural image in order to optimize the point cloud and camera parameters. The holistic SFM calculates the camera parameters of all the mural images at once, and only performs triangulation and beam leveling optimization once, so it takes the shortest time, while the hybrid SFM proposed in this paper divides the dataset into a number of subsets, and uses incremental SFM to calculate the camera parameters of the subset in each subset, and then uses the holistic SFM to solve for all the camera parameters, and then performs triangulation and beam leveling for optimization at last. Optimization, although the hybrid SFM exists the process of beam leveling several times, its running time is small compared to the incremental SFM. The reconstruction error of incremental SFM is the smallest (0-0.02), the error of integral SFM is the largest, and the reconstruction error of hybrid SFM is slightly lower than that of incremental SFM, but about 2% lower than that of integral SFM. The reason for the high reconstruction accuracy of incremental SFM is that it performs beam leveling to optimize the point cloud model and camera parameters every time a mural image is incremented. Considering the fresco digitization and conservation work, of course, the lower the error the better, and the running time difference between the three is not very big, incremental SFM is more suitable for fresco digitization heritage.

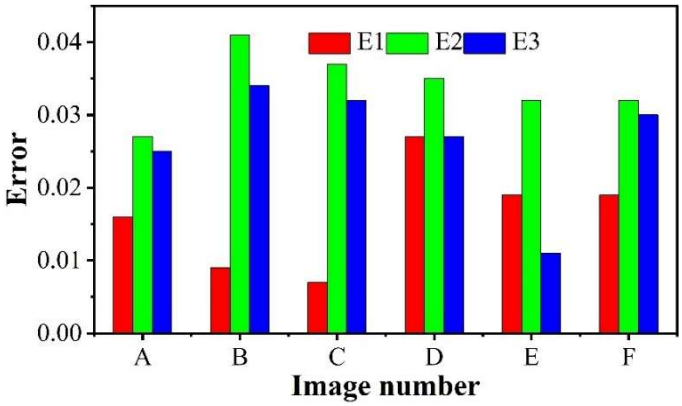

Figure 5: Comparison of errors of three types of SFM

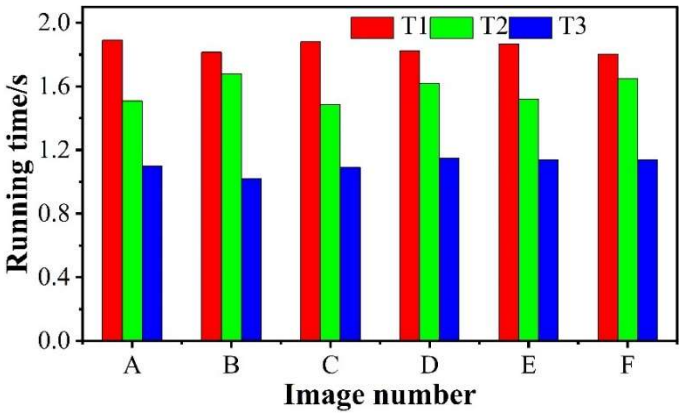

Figure 6: Comparison of the running times of three types of SFM

Figure 7 shows the number of point clouds in the sparse model obtained by the three reconstruction methods, incremental incremental image by incremental image and each incremental image triangulates the feature points once, so the number of feature points is more, and the hybrid type also uses incremental incremental incremental image by incremental image and each incremental image triangulates the feature points once in each subset, the number of point clouds of the two reconstruction methods has no big difference and the number of point clouds is about There is no big difference between the two reconstruction methods and the number of point clouds is about two times of the holistic one, the holistic one reduces the triangulated feature points by the three-view constraints, and the more the number of cloud points, the greater the authenticity of the digitized inheritance of the mural, which fully verifies the priority of the incremental SFM in the construction of sparse point clouds.

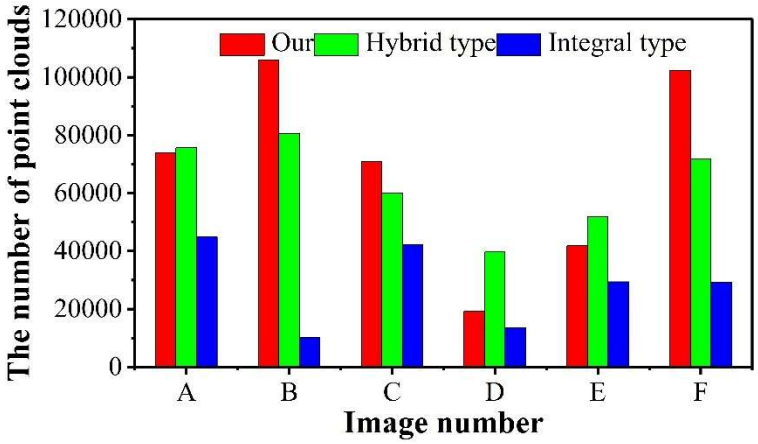

Figure 7: Three types of SFM reconstructed point cloud number

III. C. Dense point cloud analysis

In this section, the three dense reconstruction algorithms are evaluated using the mural images above, and the evaluation process mainly involves using the same incremental SFM as the input of the sparse point cloud as well as the camera bit position, and using the three algorithms to reconstruct its dense reconstruction respectively, and then comparing the number of dense point clouds generated by the three algorithms (SFS: Shadow Recovered Shape Method, C/PMVS: 3D patch expansion based algorithm, and the method in this paper: depth fusion method) to the number of dense reconstructed point clouds and runtime. The number of dense point clouds generated by the three algorithms (SFS: Shadow Recovery Shape Method, C/PMVS: 3D patch expansion based algorithm, and this paper's method: depth fusion method) are then compared, and the number of densely reconstructed point clouds versus the running time are shown in Figures 8 to 9. The results show that the texture features are not obvious when using mural images as test cases. Therefore, the number of matching points obtained during the feature extraction and matching step is high, and thus the number of reconstructed sparse point clouds is high. In dense reconstruction, both C/PMVS and depth fusion methods use sparse reconstruction as input, and the feature matching points or 3D reconstruction points are used as seed points, which are diffused according to certain rules. If the number of sparse point cloud reconstruction is high when using these two methods, the more pixel points need to be computed, the longer the time and the better the result. In this example, due to the high number of feature matches of the mural image, the depth fusion method performs better than C/PMVS, while the SFS algorithm does not rely on the results of the number of sparse reconstructed point clouds, and is only sensitive to the accuracy of the recovered camera position, but due to dense matching, the final number of reconstructed point clouds is less. Overall, the thick point cloud construction based on the depth fusion method is optimal in mural digitization heritage.

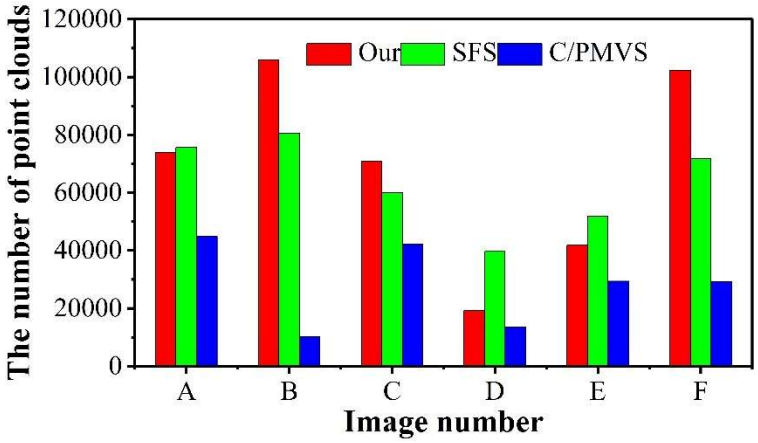

Figure 8: Comparison of the number of densely reconstructed point clouds

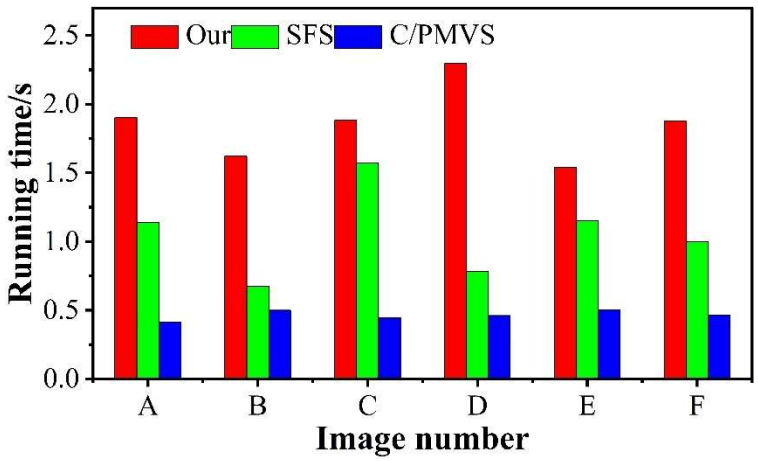

Figure 9: Comparison of the running time of dense reconstructed point clouds

III. D. Analysis of optimization effect of 3D surface modeling

In the fresco 3D surface modeling process, the error is used as the evaluation index in this subsection, and the analysis of the optimization effect of 3D surface modeling is shown in Figure 10. Before the optimization, the error of three-dimensional surface modeling of frescoes is 0.01~0.03, through the introduction of line-of-sight weights optimization operation, the existence of noise can be effectively found and can reduce the impact of noise, so that the error of three-dimensional surface modeling of its frescoes is closer to 0, and it better restores the culture of frescoes, which has a promotional effect on the digital protection and inheritance of frescoes.

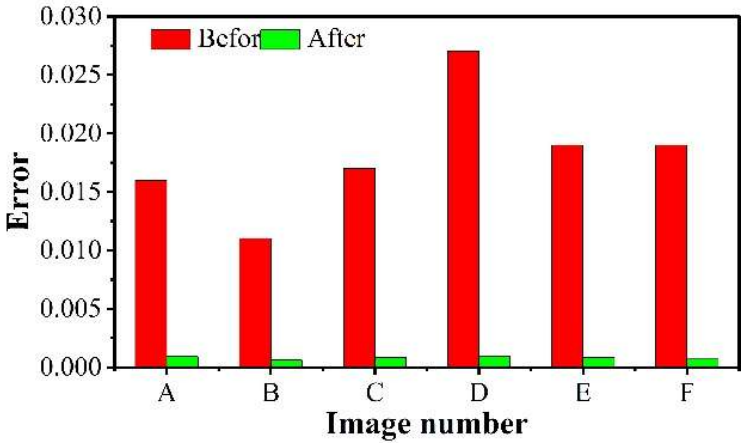

Figure 10: Analysis of the Optimization Effect of 3D Surface Modeling

III. E. Mural Texture Mapping and Rendering Analysis

Also take mural A~F as an example to explore and analyze the mural texture mapping and rendering efficiency, Fig. 11 shows the comparison of mural texture mapping time between this paper's method and traditional mural splicing technology, and Fig. 12 shows the comparison of mural rendering time between this paper's method and traditional mural splicing technology. Based on the size of the data in the figure, it can be seen that, compared with the traditional method, this paper based on three-dimensional reconstruction and texture mapping mural rapid digitization program can not only improve the quality of the mural digitization, but also in the mural texture mapping and rendering efficiency has nearly doubled, the whole aspect of this paper confirms the feasibility of the digitization of this paper program has a guiding value of reference for the promotion of the cause of the mural digitization, so that make the contemporary mural painting to be able to become a kind of art accepted by the public.

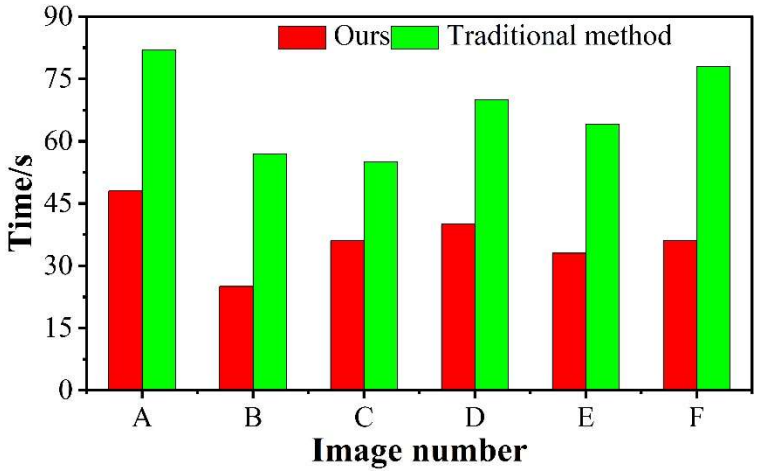

Figure 11: Comparison of mural texture mapping time

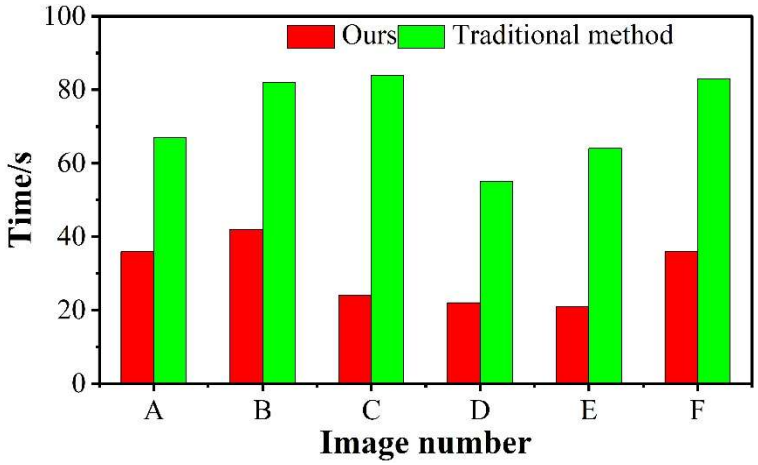

Figure 12: Comparison of mural rendering time

IV. Conclusion

In this paper, a method for digital preservation of frescoes based on texture mapping and image reconstruction techniques is proposed, and the experimental results verify the effectiveness of the scheme. It is found that in the feature matching link, the improved ISIFT algorithm achieves the minimum average error in 87 pairs of 200 pairs of fresco image samples, which is significantly better than 15 pairs of SURF algorithm, 12 pairs of SIFT algorithm and 0 pairs of ORB algorithm. The feature matching errors are almost all less than 0.0425 pixels, and the accuracy is significantly improved. In high-resolution (10244 × 7715 pixels) mural image processing, the ISIFT algorithm is able to obtain the maximum number of matching points while keeping the processing time short. In the sparse point cloud construction stage, the incremental SFM algorithm generates about twice as many point clouds as the holistic SFM, which better preserves the mural details. By introducing the line-of-sight weight optimization operation, the error of 3D surface modeling is reduced from 0.01 to 0.03 to a level close to zero. Taken together, the fresco digitization technology chain constructed in this study ensures both accurate reconstruction of geometric forms and high-fidelity restoration of texture details, providing a systematic solution for the digital preservation of frescoes. Future research will further explore multi-source data fusion and intelligent algorithm optimization to improve the robustness and efficiency of mural painting digitization in complex environments, and promote the in-depth development of cultural heritage digital preservation.

References

[1] Youzbashi, A., Hoseini, S. R., & Chareie, A. (2022). Identifying the Causes of the Emergence of Religious Themes and Its Important Components in the Murals of Religious Monuments of the Qajar Era (Case Study: Sacred Shrines of Guilan Province). Negareh Journal, 17(61), 25-47.

[2] de-Miguel-Molina, M. (2020). Visiting dark murals: an ethnographic approach to the sustainability of heritage. Sustainability, 12(2), 677.

[3] Fillis, I., & Lehman, K. (2022). Cultural murals and the evolving nature of the hero concept: an arts marketing context. Arts and the Market, 12(3), 197-214.
[4] Day, L., & Sreekala, R. (2024). Mural Making. Activating Youth As Change Agents: Integrating Youth Participatory Action Research in School Counseling, 94.
[5] Prasiasa, D. P. O. (2022). Mural art as a media for social criticism: perspective structuralist-constructivism. Mudra Jurnal Seni Budaya, 37(2), 203-211.
[6] Salim, Z. (2017). Painting a place: A spatiothematic analysis of murals in East Los Angeles. Yearbook of the Association of Pacific Coast Geographers, 79, 41-70.
[7] Rivas, T., Alonso-Villar, E. M., & Pozo-Antonio, J. S. (2022). Forms and factors of deterioration of urban art murals under humid temperate climate; influence of environment and material properties. The European Physical Journal Plus, 137(11), 1257.
[8] Mikayama, A., Hokoi, S., Ogura, D., Okada, K., & Su, B. (2019). The effects of windblown sand on the deterioration of mural paintings in cave 285, in Mogao caves, Dunhuang. Journal of Building Physics, 42(5), 652-671.
[9] Gupta, D., Singh, M., & Sawant, M. (2025). From murals to microclimate: assessing the ecological footprint of tourism at Ajanta Caves. Journal of Heritage Tourism, 20(2), 260-281.
[10] Du, R. (2025). Archaeological Analysis of Disease and Management Strategies for Murals and Oil Paintings in Labrang Monastery. Mediterranean Archaeology and Archaeometry, 25(1).
[11] Mol, V. R., & Maheswari, P. U. (2021). The digital reconstruction of degraded ancient temple murals using dynamic mask generation and an extended exemplar-based region-filling algorithm. Heritage Science, 9, 1-18.
[12] Li, Z., & Champadaeng, S. (2025). Study of Cultural Heritage and Digital Preservation: The case of Murals of the Northern Yue Temple. International Journal of Education and Literacy Studies, 13(2), 262-268.
[13] Liu, S. (2025). Research on the Conservation and Display of Mural Paintings in Tomb Chambers Based on Digital Twin Technology. J. COMBIN. MATH. COMBIN. COMPUT, 127, 2429-2442.
[14] Hu, X., Ng, J., Xia, S., & Fu, Y. K. Y. (2017). Evaluating metadata schema for murals and stone cave temples: Towards digitizing cultural heritage. Proceedings of the Association for Information Science and Technology, 54(1), 491-494.
[15] Zhou, X., Yang, Y., & Yan, D. (2025). Research on Digital Orthophoto Production Technology for Indoor Murals in the Context of Climate Change and Environmental Protection. Journal of Imaging, 11(5), 140.
[16] Kong, Q., & Qiao, Y. (2022). Research and Application of Color of Qiuci Murals Based on Intelligent Digital Image Processing Technology. Wireless Communications and Mobile Computing, 2022(1), 5853561.
[17] Li, N., Gong, X., Li, H., & Jia, P. (2018). Nonuniform multiview color texture mapping of image sequence and three-dimensional model for faded cultural relics with sift feature points. Journal of Electronic Imaging, 27(1), 011012-011012.
[18] Kharfouchi, K., Labii, B., Hamma, W., AOU, H. A., & Kharfouchi, S. (2024). AN INNOVATIVE APPROACH TO AUTOMATED TEXTURE MAPPING FOR ARCHITECTURAL HERITAGE PRESERVATION. Urbanism. Architecture. Constructions/Urbanism. Arhitectura. Constructii, 15(1).
[19] Wang, L., Wang, Z., Wang, Y., Huang, G., Xing, Y., Yang, F., ... & Niu, S. (2025). Surface whitening prevention strategy of the mural relics from consolidation treatment: An innovative calcium protectant. Chemical Engineering Journal, 510, 161276.
[20] Gomoiu, I., Cojoc, R., Ruginescu, R., Neagu, S., Enache, M., Dumbrăvician, M., ... & Ghervase, L. (2022). The susceptibility to biodegradation of some consolidants used in the restoration of mural paintings. Applied Sciences, 12(14), 7229.
[21] Refaat, F., Marey Mahmoud, H., El-Sabbagh, B., & Brania, A. (2020). Evaluating thermal and UV stability of some protective coatings for historical murals in Egypt. Advanced research in conservation science, 1(2), 31-47.
[22] Priego, E., Herráez, J., Denia, J. L., & Navarro, P. (2022). Technical study for restoration of mural paintings through the transfer of a photographic image to the vault of a church. Journal of Cultural Heritage, 58, 112-121.
[23] Muralidhar, S., & Bhardwaj, A. (2024). Preservation and Archiving of Historic Murals Using a Digital Non-Metric Camera. Engineering Proceedings, 82(1), 60.
[24] Gao, Z., Du, M., Cao, N., Hou, M., Wang, W., & Lyu, S. (2023). Application of hyperspectral imaging technology to digitally protect murals in the Qutan temple. Heritage Science, 11(1), 8.
[25] Tian, X., & Ding, X. (2025). Optimisation of digital preservation and 3D reconstruction of frescoes based on image processing algorithms. J. COMBIN. MATH. COMBIN. COMPUT, 127, 449-468.
[26] Krittachai Boonsivanon & Worawat Sa Ngiamvibool. (2021). A SIFT Description Approach for Non-Uniform Illumination and Other Invariants. ISI,26(6),533-539.
[27] Lihong Yang,Shunqin Xu,Zhiqiang Yang,Jia He,Lei Gong,Wanjun Wang... & Zhili Chen. (2025). Fast Registration Algorithm for Laser Point Cloud Based on 3D-SIFT Features. Sensors,25(3),628-628.
[28] Lei Liu,Congzheng Wang,Chuncheng Feng,Wanqi Gong,Lingyi Zhang,Libin Liao & Chang Feng. (2024). Incremental SFM 3D Reconstruction Based on Deep Learning. Electronics,13(14),2850-2850.